Signal Shaping for Unique-Word OFDM by Selected Mapping

Johannes B. Huber*, Jakob Rettelbach*, Mathis Seidl*, and Mario Huemer†
*Institute for Information Transmission, Universität Erlangen-Nürnberg, Erlangen, Germany
Email: {seidl, huber}@LNT.de, Telephone: +49 9131 85-27112
†Institute of Networked and Embedded Systems, University of Klagenfurt, Austria
Email: mario.huemer@aau.at, Telephone: +43 463 2700-3660

***Abstract*—Selected Mapping (SLM) is known to be a useful method to reduce the peak to average power ratio (PAPR) of OFDM transmit signals. In this paper, the performance of PAPR-reduction for Unique Word (UW-) OFDM is investigated where in contrast to usual cyclic prefix (CP-) OFDM correlations between subcarrier data exist due to a complex number Reed-Solomon code along the subcarriers. It is shown that these correlations do not impair the positive properties of SLM for PAPR-reduction. Moreover, SLM is a general method for shaping of transmit signals generated in blocks in order to strengthen some desired signal features and e.g. may be applied to lower efficiently the average power of the redundant subcarriers in UW-OFDM. Furthermore, we show that SLM together with UW-OFDM is well suited for reducing the peak to minimum ratio (PMR) of the transmit signal as well. Analytic results are accompanied by simulation results.**

I. Introduction

In [1], [2] we introduced an OFDM signaling scheme, where the usual cyclic prefixes (CP) are replaced by deterministic sequences that we call unique words (UW). (A related but – when regarded in detail – very different scheme is KSP (known symbol padded)-OFDM [3], [4].)

In CP- as well as in UW-OFDM the linear convolution of the transmit signal with the channel impulse response is transformed into a cyclic convolution. However, there are some fundamental differences between the CP-based and the UW-based approach:

- Different to the CP, the UW is part of the DFT (discrete Fourier transform) interval.
- The CP is a random sequence, whereas the UW is deterministic. Thus, the UW can optimally be designed for particular needs like synchronization and/or channel estimation purposes at the receiver side.

The insertion of the UW within the DFT interval introduces a complex number Reed-Solomon (RS) code (or a coset of an RS code, resp.), i.e. specific correlations in the frequency domain, which can advantageously be exploited by the receiver to improve the BER (bit error ratio) performance, cf. [5], [6]. In our concept described in [1] we suggest to generate at first an all-zero block in time domain by appropriately loading so-called redundant subcarriers in which subsequently a proper UW is inserted. A minimization of the energy contribution of the redundant subcarriers turned out to be a challenge. For this purpose, at first the positions of the redundant subcarriers have to be optimized, cf. [1]. One goal of this paper is to show that Selected Mapping (SLM) can efficiently be employed for further reduction of energy of the redundant subcarriers.

The paper is organized as follows: Sections 2 and 3 give short reviews on signal generation and encoding for unique word (UW-) OFDM and on the principle of signal shaping by means of SLM as well. In Section 4, the reduction of average energy for redundant subcarriers is discussed, both, in a rather simplified model for an analytic approach and in a simulation study in order to estimate the effects due to simplifications. Because of the correlations among the subcarriers introduced by the complex-number RS encoding, the well known theory for performance analysis of SLM for classical peak to average power reduction (PAPR-R) as given in [7], [8] is not applicable to UW-OFDM in a straight forward way. As an analytic approach seems not to be feasible for UW-OFDM, we present a simulation study of PAPR-R by SLM and give a comparison to CP-OFDM in Section 5. By this we show that – despite of RS encoding – SLM is as powerful in PAPR-R for UW-OFDM as for CP-OFDM. In section 6, reduction of the peak-to-minimum ratio (PMR) of transmit signals is addressed. The paper finishes with conclusions in Section 7.

Notation: Lower-case bold face variables ($\mathbf{a}, \mathbf{b}, \dots$) indicate vectors, and upper-case bold face variables ($\mathbf{A}, \mathbf{B}, \dots$) indicate matrices. To distinguish between time and frequency domain variables, we use a tilde to express frequency domain vectors and matrices ($\tilde{\mathbf{a}}, \widetilde{\mathbf{A}}, \dots$), respectively. We further use $\mathbb{C}$ to denote the set of complex numbers with j being the imaginary unit, $\mathbf{I}$ to denote the identity matrix, $(\cdot)^T$ to denote transposition, $(\cdot)^H$ to denote conjugate transposition, $E[\cdot]$ to denote expectation, and $\mathrm{tr}(\cdot)$ to denote the trace operator. For all signals and systems the usual equivalent complex baseband representation is applied.

II. Review of UW-OFDM: Unique Word Generation with SLM

We briefly review our approach of introducing unique words in OFDM time domain symbols, for further details see [1], [2]. Let $\mathbf{x}_u \in \mathbb{C}^{N_u \times 1}$ be a predefined sequence which we call unique word. This unique word shall form the tail of each OFDM time domain symbol vector $\mathbf{x} = \begin{bmatrix}\mathbf{x}_d^T & \mathbf{x}_u^T\end{bmatrix}^T \in \mathbb{C}^{N \times 1}$, whereas only $\mathbf{x}_d \in \mathbb{C}^{(N-N_u)\times 1}$ is random and affected by the data to be transmitted. In the concept of [1], [2] we propose to generate an OFDM symbol $\mathbf{x} = \begin{bmatrix}\mathbf{x}_d^T & \mathbf{0}^T\end{bmatrix}^T$ with a zero block in a first step, and to assemble the final transmit symbol $\mathbf{x}' = \mathbf{x} + \begin{bmatrix}\mathbf{0}^T & \mathbf{x}_u^T\end{bmatrix}^T$ by adding the desired UW. As in conventional OFDM, QAM data symbols (denoted by the vector $\tilde{\mathbf{d}} \in \mathbb{C}^{N_d \times 1}$) and some zero subcarriers (as usual at the band edges and at DC) form a part of the vector $\tilde{\mathbf{x}}$ in frequency domain, but here in addition the zero block is specified in time domain as part of the vector $\mathbf{x} = \mathbf{F}_N^{-1}\tilde{\mathbf{x}}$. Here, $\mathbf{F}_N$ denotes the length-N DFT matrix with elements $[\mathbf{F}_N]_{kl} = \mathrm{e}^{-\mathrm{j}\frac{2\pi}{N}kl}$ for $k, l = 0, 1, ..., N-1$. The system of equations $\mathbf{x} = \mathbf{F}_N^{-1}\tilde{\mathbf{x}}$ can be fulfilled by introducing a set of redundant subcarriers. The redundant subcarrier symbols form the vector $\tilde{\mathbf{r}} \in \mathbb{C}^{N_r \times 1}$ with $N_r = N_u$. We further introduce a permutation matrix $\mathbf{P} \in \mathbb{C}^{(N_d+N_r)\times(N_d+N_r)}$ for the frequency domain vector in order to shift the redundant subcarriers to its optimum positions. Thus, an OFDM symbol is formed in frequency domain by $\tilde{\mathbf{x}} = \mathbf{B}\mathbf{P}\left[\begin{smallmatrix}\tilde{\mathbf{d}}\\ \tilde{\mathbf{r}}\end{smallmatrix}\right]$. Here, $\mathbf{B} \in \mathbb{C}^{N\times(N_d+N_r)}$ models the insertion of $N - N_d - N_r$ zero subcarrier symbols. By this, the time–frequency relation $\mathbf{F}_N^{-1}\tilde{\mathbf{x}} = \mathbf{x}$ reads

$$\mathbf{F}_N^{-1}\mathbf{B}\mathbf{P}\begin{bmatrix}\tilde{\mathbf{d}}\\ \tilde{\mathbf{r}}\end{bmatrix} = \begin{bmatrix}\mathbf{x}_d\\ \mathbf{0}\end{bmatrix}. \quad (1)$$

With $\mathbf{M} = \mathbf{F}_N^{-1}\mathbf{B}\mathbf{P} = \left[\begin{smallmatrix}\mathbf{M}_{11} & \mathbf{M}_{12}\\ \mathbf{M}_{21} & \mathbf{M}_{22}\end{smallmatrix}\right]$, where $\mathbf{M}_{kl}$ are appropriate sized sub-matrices, it follows that $\mathbf{M}_{21}\tilde{\mathbf{d}} + \mathbf{M}_{22}\tilde{\mathbf{r}} = \mathbf{0}$, and hence $\tilde{\mathbf{r}} = -\mathbf{M}_{22}^{-1}\mathbf{M}_{21}\tilde{\mathbf{d}}$. With the matrix $\mathbf{T} = -\mathbf{M}_{22}^{-1}\mathbf{M}_{21} \in \mathbb{C}^{N_r \times N_d}$, the vector of redundant subcarrier symbols can thus be determined by the linear mapping $\tilde{\mathbf{r}} = \mathbf{T}\tilde{\mathbf{d}}$. The energies of the redundant subcarrier symbols highly depend on the choice of $\mathbf{P}$ and the minimization of the mean redundant energy contribution corresponds to solving the optimization problem $\mathbf{P} = \mathrm{argmin}\{\mathrm{tr}(\mathbf{Q})\}$ with $\mathbf{Q} = \mathbf{T}\mathbf{T}^H$. An example of the optimum redundant subcarrier distribution for a specific parameter setup is given below. In the following, we use the notation $\tilde{\mathbf{c}}$ with

$$\tilde{\mathbf{c}} = \mathbf{P}\begin{bmatrix}\tilde{\mathbf{d}}\\ \tilde{\mathbf{r}}\end{bmatrix} = \mathbf{P}\begin{bmatrix}\mathbf{I}\\ \mathbf{T}\end{bmatrix}\tilde{\mathbf{d}} = \mathbf{G}\tilde{\mathbf{d}}, \quad (2)$$

whereas the matrix $\mathbf{G} = \mathbf{P}\begin{bmatrix}\mathbf{I} & \mathbf{T}^T\end{bmatrix}^T \in \mathbb{C}^{(N_d+N_r)\times N_d}$ can be interpreted as a code generator matrix for a systematic complex valued Reed Solomon code, that generates the code words $\tilde{\mathbf{c}}$.

Fig. 1 shows a block diagram of the UW-OFDM signal generation employing SLM (scrambling method, see [9] and next section). The processing at the transmitter side starts with generation of V different representations of the data, e.g. by means of different ways of enscrambling of data. In each of the V data blocks, the way of modification of original data is encoded by means of $\log_2(V)$ redundant binary symbols. In each branch (outer) channel encoding, short intraframe interleaving and QAM mapping follow.

Next, the redundant subcarrier symbols are determined. After assembling the OFDM symbol in frequency domain, which is composed of $\tilde{\mathbf{d}}$, $\tilde{\mathbf{r}}$, and a set of zero subcarriers, the IFFT is computed. All V versions of the transmit signal $\mathbf{x}$ in time domain are analyzed with respect to the feature which one wants to improve (i.e. signal shaping) by means of SLM, and that one signal is selected for transmission which exhibits the most advantageous properties. Finally, the UW is added in time domain.

For simulation results we compare the UW-OFDM approach with the CP-OFDM based IEEE 802.11a WLAN standard [10], i.e. we use a parameter setup which is adapted to the 802.11a standard wherever possible, cf. [1]: $N = 64$, sampling frequency $f_s = 20$MHz, DFT period $T_{DFT} = 3.2\mu$s, guard duration $T_{GI} = 800$ns, QPSK as modulation scheme, subcarrier spacing $\Delta f = 312.5$ kHz, $N_r = N_u = 16$, $N_d = 36$. The indices of the zero subcarriers within an OFDM symbol $\tilde{\mathbf{x}}$ are set to {0, 27, 28,...,37}. The indices of the redundant subcarriers are chosen to be {2, 6, 10, 14, 17, 21, 24, 26, 38, 40, 43, 47, 50, 54, 58, 62}. This set (which is expressed by an appropriate permutation matrix $\mathbf{P}$) minimizes the energy of the redundant subcarriers on average.

III. Signal Shaping by means of Selected Mapping

The method Selected Mapping (SLM) has been introduced in [7] for peak to average power ratio reduction (PAPR-R) in OFDM transmit signals. The idea of SLM is to produce several, i.e. V, different versions of a transmit signal which represent the same vector of data symbols for the receiver. In the original idea of [7], different phase factors were proposed to be multiplied per component to QAM data symbols at the subcarriers of OFDM. Many further proposals to modify a signal in order to generate different representations of the same data vector had been published later on, cf. [11]. Out of these different signals, the one with the smallest peak value in time domain is selected. By this, the probability of a severe overload of the high power amplifier (HPA) at the transmitter at a certain Back-Off can be drastically reduced resulting in a lower level of spectral side lobes generated by nonlinear limitation effects within the HPA. Thus, for satisfying standardized spectral masks of the HPA, a smaller Back-Off my be chosen resulting in a rather increased power efficiency of the communication scheme. The price to be paid for this advantage is a redundancy of $\log_2(V)$ bit which have to be transmitted as side information specifying the actual selected mapping of data to signal. As only a few different representations are desirable because of complexity constraints and which usually are indeed sufficient (i.e. $V \leq 16$) for an effective PAPR-R, only a very small amount of redundancy is introduced by SLM (i.e. up to 4 bit out of usually hundreds of bit usually transmitted by one OFDM frame). In [9] we proposed a special version of SLM employing a usual scrambler for the binary data to be transmitted, i.e. a pure recursive IIR system in the binary field, in front of the OFDM modulation scheme. Different versions of transmit signals are generated by different pre-initializations of the memory elements (D-Flip-Flops) of the scrambler before scrambling the data of one OFDM frame. At the receiver side, the corresponding descrambler is a pure FIR system and the initialization of the scrambler simply

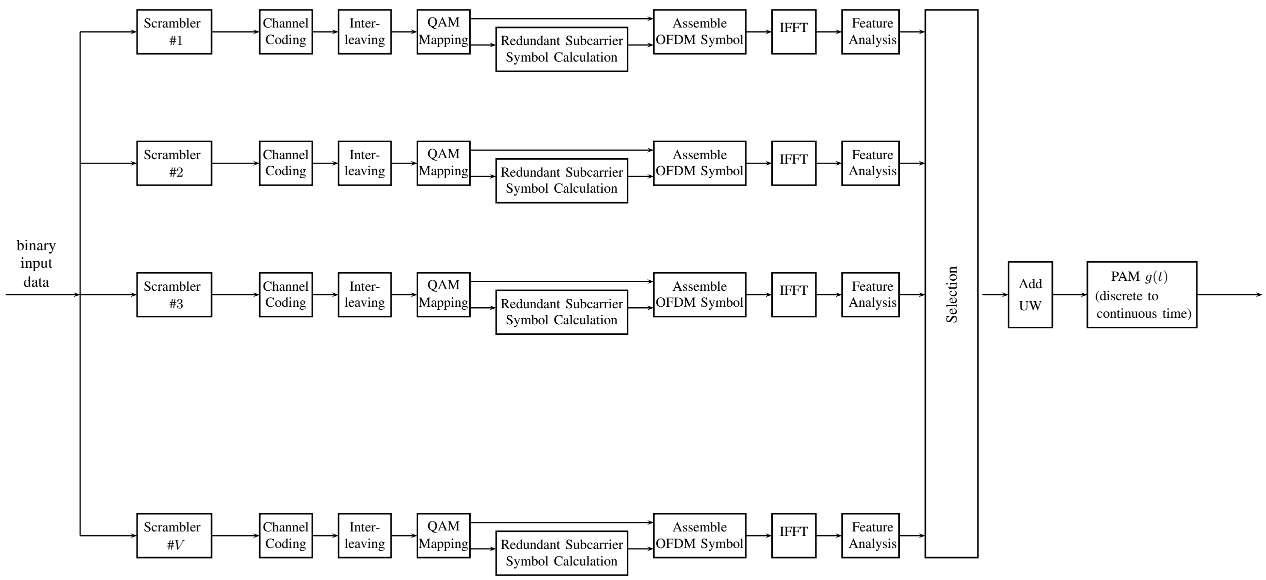

Fig. 1. Block diagram of signal generation for SLM with UW-OFDM

corresponds to the first $\log_2(V)$ descrambled data symbols. Thus, this favourite version of SLM does not need any explicit transmission of side information and there is no catastrophic error propagation in case of an erroneous side information.

SLM cannot only be employed for PAPR-R of an OFDM transmit signal but for improvement of any desired feature of an information representing signal, e.g. for single carrier or baseband transmission as well, as long as a generation of the transmit signal in independent subsequent blocks is implementable. Thus SLM, especially in its scrambler variant, is a general method for signal shaping by introduction of a small amount of redundancy. In [8] it is shown, that for PAPR-R of OFDM, SLM is quite close to an existence bound from information theory for the trade-off between reduction of peak power and introduced redundancy and therefore it is hard to be outperformed. If the desired feature can be expressed by means of a real variable χ – which is desired to be as low as possible – the behaviour of a modulation scheme with respect to this parameter χ which usually depends on the actual data to be transmitted and therefore is a random variable, is favourably expressed by means of a complementary cumulative distribution function (CCDF) $C(x) = \Pr(\chi > x)$. (Note that for PAPR-R the parameter χ should correspond to the peak power value within the actual block and not PAPR itself. In literature, several proposals of "successful" PAPR-R can be found where the reduction is more due to an increase of average power (i.e. the denominator of PAPR) than a decrease of peak power which, of course, is counterproductive for technical practice.) The corresponding limit x for parameter χ is exceeded in case of SLM if it is exceeded for all V versions which are offered for selection. Thus, if these versions can be viewed as statistically independent blocks of data, the resulting CCDF $C_{\mathrm{SLM}}(x)$ is simply given by $C_{\mathrm{SLM}}(x) = (C(x))^V$.

Example: We consider a vector of length N of i.i.d. complex valued Gaussian variables with normalized variance 1 to model the discrete time domain signal in cyclic prefix CP-OFDM (justification: central limit theorem and the unitary discrete Fourier transform matrix $\mathbf{F}_N$). The probability density function (pdf) $f_x(x)$ of the actual power of the ith vector component is given by $f_x(x) = \mathrm{e}^{-x}$ for $x \geq 0$ with CDF $F_x(x) = 1 - \mathrm{e}^{-x}$. Thus, the CCDF for the maximum power $\chi := \max_i |x_i|^2$ within a vector reads:

$$C(x) = \Pr(\chi > x) = 1 - (F_x(x))^N.$$

Therefore, the equation

$$C_{\mathrm{SLM}}(x) = (1 - (1 - \mathrm{e}^{-x})^N)^V$$

is a simple model for the behaviour of SLM (i.i.d. complex valued Gaussian random variables in all components of all mutually independent mappings) and may be used for performance comparisons.

IV. Reduction of Energy of Redundant Subcarrier Symbols

The redundant subcarrier symbols are calculated from the N_d data symbols by $\tilde{\mathbf{r}} = \mathbf{T}\tilde{\mathbf{d}}$, see Section 2, and therefore are random. For i.i.d. data symbols with variance σ_d^2 the mean sum energy is given by $\sigma_d^2 \cdot \mathrm{tr}(\mathbf{Q})$.
Note that for our simulation example $\mathrm{tr}(\mathbf{Q}) = 36.57$ holds, i.e. on average the redundant symbols have more than twice the energy of that of the data symbols. In order to lower the energy of redundant symbols we propose to take the actual sum energy $\tilde{\mathbf{r}}_v^H \tilde{\mathbf{r}}_v$ of version v as a selection criterion in an SLM approach which results in an increased power efficiency of the

scheme due to signal shaping. Assuming perfect scrambling for generation of different versions of the transmit signal, cf. Fig. 1, an analytic approach for analysis of the scheme would be possible if the CCDF $C_r(x) = \Pr(\tilde{\mathbf{r}}^H\tilde{\mathbf{r}} \geq x)$ is available. Following central limit theorem arguments (i.e. a redundant symbol is generated by a weighted sum of N_d i.i.d. data symbols), the joint pdf of all N_r complex valued redundant symbols r_i may be well modeled by the joint pdf of N_r complex valued Gaussian variables with zero mean and covariance matrix $\mathbf{Q}$:

$$f_r(\mathbf{r}) = \frac{1}{\pi^{N_r}|\det(\mathbf{Q})|} \cdot \exp(-\mathbf{r}^H\mathbf{Q}^{-1}\mathbf{r})$$

Since the matrix $\mathbf{Q}$ contains non-zero off-diagonal elements and non-identical diagonal elements, the standard analytic approach for calculation of a CDF for $\mathbf{r}^H\mathbf{r}$ by a transform from Cartesian to polar coordinates is not possible in a direct way, like it is usual for considering Chi-Square distributed random variables. A numerical evaluation, i.e. a numerical integration in N_r dimensions over a sphere with radius $\sqrt{x}$ also does not seem to be feasible. For a first approximation we decided simply to ignore the off-diagonal elements in $\mathbf{Q}$, i.e. assuming uncorrelated redundant subcarrier symbols. Taking the complex Gaussian model, the pdf $p_i(x)$ for the energy $x = |r_i|^2$ of the i-th redundant subcarrier symbol is simply given by

$$p_i(x) = a_i \mathrm{e}^{-a_i x} \quad , \quad a_i > 0$$

where a_i denotes the inverse of the i-th element on the main diagonal of the covariance matrix $\mathbf{Q}$ (i.e. $a_i = 1/q_{ii}$), as well known for Rayleigh distributed random variables, see e.g. [12]. As long as we assume no correlations and by this statistical independence (Gaussian model) among the symbols r_i, the pdf of the sum $\mathbf{r}^H\mathbf{r}$ results in an $(N_r - 1)$-fold convolution of the pdf's $p_i(x)$ corresponding to the product of its Fourier transforms $P_i(f)$ (characteristic functions) with

$$P(f) = \prod_{i=1}^{N_r} P_i(f) \ ,$$
$$P_i(f) = \mathcal{F}(p_i(x)) = \frac{a_i}{a_i + \mathrm{j}2\pi f}$$

We assume that all a_i are (at least slightly) mutually different[1], therefore a usual expansion into partial fractions can be applied:

$$P(f) = \sum_{i=1}^{N_r} \frac{A_i}{a_i + \mathrm{j}2\pi f} \quad ,$$

$$A_i = \frac{\mathrm{j}2\pi \prod_{l=1}^{N_r} a_l}{\frac{\mathrm{d}}{\mathrm{d}f}\left(\prod_{l=1}^{N_r}(a_l + \mathrm{j}2\pi f)\right)\Big|_{f=\mathrm{j}\frac{a_i}{2\pi}}}$$

[1]If indeed two variables a_i are exactly equal, we artificially introduce a slight deviation for numerical evaluations. Of course, multiple poles may also be taken into consideration as usual.

Thus, the pdf $s(x)$ of the sum $\mathbf{r}^H\mathbf{r}$ can be expressed as a sum of one-sided exponential functions

$$s(x) = \sum_{i=1}^{N_r} A_i \mathrm{e}^{-a_i x} \quad , \quad x \geq 0$$

and its corresponding CCDF $C'_r(x)$ reads

$$C'_r(x) = \sum_{i=1}^{N_r} \frac{A_i}{a_i}\ \mathrm{e}^{-a_i x} \quad , \quad x > 0$$

Fig. 2 and Fig. 3 show pdf's and CCDF's of the sum energy

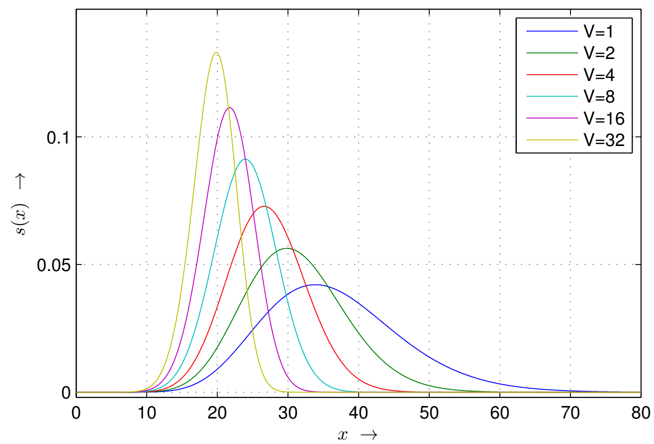

Fig. 2. Analytically derived pdf's of the sum energy of redundant subcarrier symbols for UW-OFDM and SLM with varying parameter V

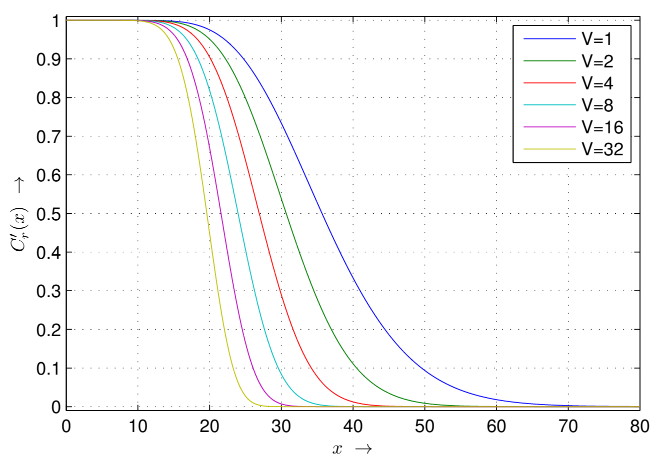

Fig. 3. CCDF's of the sum energy of redundant subcarrier symbols for UW-OFDM corresponding to Fig. 2

of redundant subcarrier symbols for this Gaussian model of uncorrelated redundant subcarrier symbols, where the system setup discussed in Section 3 is applied. As outlined in Section 3, the CCDF has to be taken to the power V if SLM is applied to lower this energy, corresponding curves are given in Fig. 3 for $V = 2, 4, 8, 16, 32$ as well. The corresponding pdf's of Fig. 2 are calculated from these CCDF's by means of numerical differentiation and the mean energy E_V of all

TABLE I
ANALYTICALLY DERIVED GAINS OF UW-OFDM WITH SLM OVER PLAIN UW-OFDM

V	1	2	4	8	16	32
E_V	36.53	31.09	27.06	23.97	21.51	19.50
G_{SLM} (w/o rate loss) (dB)	–	0.34	0.61	0.83	1.01	1.16
G_{SLM} (dB)	–	0.28	0.49	0.64	0.76	0.85

TABLE II
SIMULATED GAINS OF UW-OFDM WITH SLM OVER PLAIN UW-OFDM

V	1	2	4	8	16
E_V	36.57	31.99	28.43	25.58	23.23
G_{SLM} (w/o rate loss) (dB)	–	0.28	0.52	0.71	0.88
G_{SLM} (dB)	–	0.22	0.39	0.53	0.63

redundant symbols is determined from these pdf's. Table I shows that one might expect a decrease of the mean energy of redundant subcarrier symbols almost by a factor of 2 due to SLM. Together with the N_d active subcarrier symbols, for which an M-ary modulation scheme with variance σ_d^2 per subcarrier is assumed (here $N_d = 36$, QPSK, $\sigma_d^2 = 1$), the gain in power efficiency due to SLM reads

$$G_{\mathrm{SLM}} = -10\log_{10}\Big(\frac{E_V + N_d}{\mathrm{tr}(\mathbf{Q}) + N_d}\Big) + 10\log_{10}\Big(\frac{N_d\log_2(M) - \log_2(V)}{N_d\log_2(M)}\Big). \quad (3)$$

The second term in (3) corresponds to the rate loss for transmission of the actual selected mapping from data to transmit signal as an (perhaps non-explicit) side information. In Table I estimates for the overall gain are shown for the system setup introduced in Section 1, too.
Because of the crude simplification of the analysis above a simulation study of the scheme outlined in Section 1 had been performed. In Fig. 4, the empirical CCDF obtained by simulations is shown. A comparison with Fig. 3 already indicated that the model neglecting correlations between subcarrier symbols (i.e. neglecting off main diagonal elements in $\mathbf{Q}$) is optimistic. The variance of the sum energy of redundant subcarrier symbols is smaller due to these correlations (to be seen as a steeper descent of the CCDF). Thus, the real gain in Fig. 4 when compared to Fig. 3 is somewhat smaller than predicted from the simplified analysis, see Table II. But nevertheless, SLM is a useful tool to lower the energy for redundant subcarrier symbols in UW-OFDM and the simplified analysis presented above may help for a first estimation of possible gains. It has to be mentioned that the gain in average power efficiency due to SLM for redundant subcarrier symbols decreases for increasing length of OFDM frames together with its UW-prefix, because the standard deviation of energy in redundant symbols will become smaller in relation to its expectation. Thus, the proposed method is advantageous especially for short OFDM frames. This is in contrast to PAPR-R by SLM.

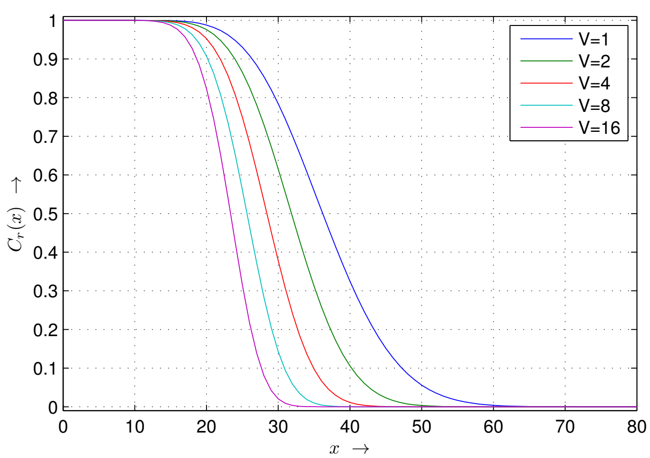

Fig. 4. Simulated CCDF's of the sum energy of redundant subcarrier symbols for UW-OFDM

V. PAPR-REDUCTION FOR UW-OFDM BY SLM

As shown in Section 2, besides the vector $\tilde{\mathbf{d}}$ of i.i.d. data symbols we have the vector $\tilde{\mathbf{r}}$ of the redundant subcarriers at optimized positions which is generated via $\tilde{\mathbf{r}} = \mathbf{T}\tilde{\mathbf{d}}$. In contrast to CP-OFDM, there are strong correlations between data symbols and redundant subcarrier symbols and also among these subcarrier values due to this linear encoding rule. Additionally, the powers of the redundant subcarriers vary significantly and are different from that of data symbols. Thus, a simple model of i.i.d. complex Gaussian random variables in time domain no longer is as well justified as for CP-OFDM. Therefore, it has to be investigated how PAPR-R by means of SLM performs in UW-OFDM. An analytic approach would require an N-fold integration over a joint pdf of N complex valued mutually correlated variables. Even under the assumption that the Gaussian model would be still valid, this seems to be an intractable task. Thus, in order to find the CCDF $C(x)$ of the T-spaced random values in time domain, we decided in favour of a study by means of simulations. As indicated in Section 2, we take the example of a UW-OFDM system corresponding to the CP-OFDM scheme of the IEEE 802.11.a wireless LAN standard. Fig. 5 shows the relative frequencies of breaking a limit x of peak power in the T-spaced discrete time signal within the 52 non-zero samples after IFFT. The block of the UW is not taken into this analysis because a proper choice of a UW is completely independent of the SLM procedure, see Fig. 1. The results show that at a very low threshold x UW-OFDM performs worse than the model of i.i.d. complex Gaussian samples. But in the region of interest, e.g. at $C(x) \leq 10^{-3}$ which corresponds to a strict limitation of out-of-bound power radiation, SLM for UW-OFDM shows a quite similar behaviour as this model, mostly even better. Moreover, UW-OFDM never gives worse results for PAPR-R when compared to CP-OFDM. This result is illustrated by the example of Fig. 6, too, where the magnitudes of the discrete time signals with and without SLM ($V = 16$) are compared for one snapshot. The results clearly indicate that PAPR-R can be

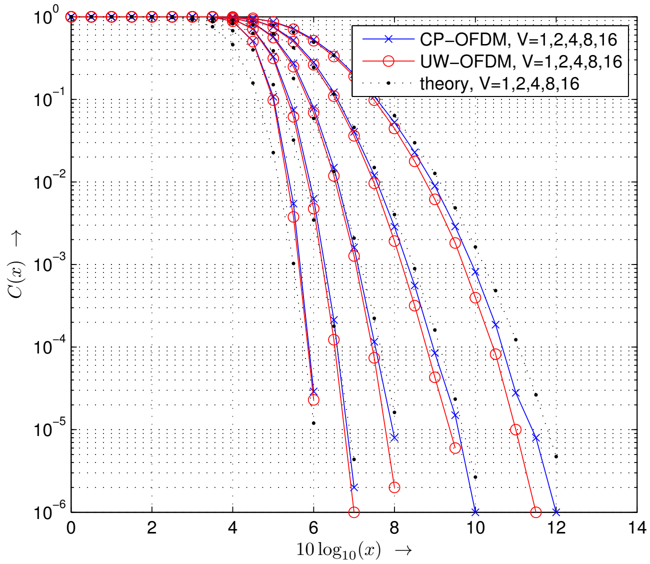

Fig. 5. Simulated CCDF of the PAPR for SLM together with CP-OFDM, UW-OFDM as well as theoretical results assuming i.i.d. complex Gaussian random variables

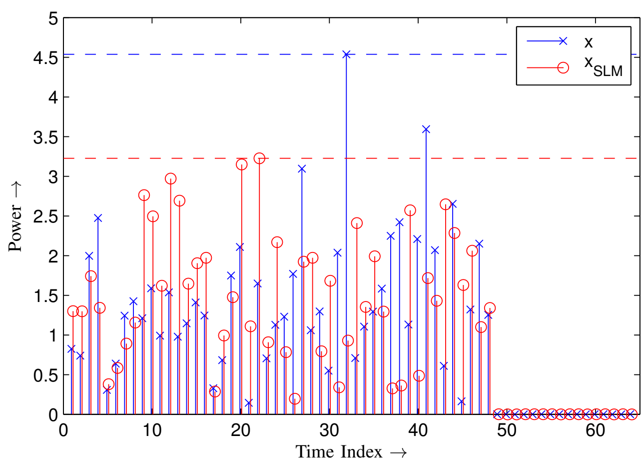

Fig. 6. Snapshot of the power values of the discrete time signals for UW-OFDM with and without SLM for PAPR reduction ($V = 16$)

employed for UW-OFDM in the same way as for CP-OFDM with comparable savings in peak power.

VI. PMR-Reduction by Selected Mapping

For efficient high power amplifiers (HPA) of digital communication systems not only a great PAPR but also signal values with a very small magnitude should be avoided. E.g. in modern concepts for design of highly power efficient HPA, a splitted processing for magnitude (AM) and phase (PM) of the RF-signal is applied allowing binary signal processing (switching) of the PM component at carrier frequency whereas the AM component remains restricted to a bandwidth which corresponds to the baud rate of the data signal. For such a splitting, a transform of signal samples in equivalent complex baseband processing from IQ-representation (i.e. real part, imaginary part) into polar coordinates has to be implemented [13]. As the phase variable in polar coordinates exhibits very fast changes for samples with low magnitude, the bandwidth of the phase signal is almost unlimited as long as zero crossings of the transmit signal in equivalent complex baseband domain exist. Therefore, RF-engineers are interested as well in the peak to minimum power ratio (PMR) as in PAPR of a transmit signal. As Selected Mapping is a very general method of signal shaping this method can be employed for PMR-reduction (PMR-R) in an analogous way as for PAPR-R simply by changing the selection criteria.

Denote the samples in time domain in an OFDM scheme after IFFT by $\mathbf{x} = (x_1, \ldots, x_n)$. PMR of this vector is defined by

$$PMR = \max_{i,j} \frac{|x_i|^2}{|x_j|^2} = \frac{\max_i |x_i|^2}{\min_j |x_j|^2} =: \frac{\max_i u_i}{\min_j u_j} \tag{4}$$

with $u_i = |x_i|^2$.

One possibility of PMR-R is to use a variable PMR_v of the v-th version of signal generation in a Selected Mapping setup directly for selection. Alternatively any other sort of nonlinear processing of $\max_i u_i$ and $\min_i u_i$ to form a combined metric in order to avoid both high peak and very low minimum power may be used resulting in different effective PMR.

As shown in section 3, the performance of an SLM procedure can be estimated by a CCDF for the parameter to be minimized. Here we give a simplified calculation of a CCDF of PMR according to eq. (4), assuming uncorrelated complex-valued Gaussian random variables in vector $\mathbf{x}$ in time domain. This assumption seems to be more appropriate to CP-OFDM but results of section 4 indicate that the behavior of UW-OFDM will not essentially differ from that for CP-OFDM. For CP-OFDM, it is widely accepted that the components x_i can be modeled to be i.i.d. with pdf $\mathcal{N}_c(0, \sigma^2 = 1)$ which corresponds to components $u_i = |x_i|^2$ being i.i.d. with pdf $f_u(u) = \mathrm{e}^{-u}$. Under these conditions holds:

$$\begin{aligned}\Pr(\min_i u_i \le z) &= 1 - \Pr(\min_i u_i > z)\\ &= 1 - \Big(\Pr(u > z)\Big)^n\\ &= 1 - \mathrm{e}^{-nz}\ .\end{aligned} \tag{5}$$

Thus, the pdf of $\min_i u_i$ is given by

$$f_{\min}(z) = n \cdot e^{-nz}. \tag{6}$$

Let $i_{\min} = \arg\min_i u_i$ and $u_{i_{\min}} = z$. Then, the conditional pdf for each of the residual $n-1$ components is given by

$$f_u(u|z) = \begin{cases} 0 & , \ u < z \\ \mathrm{e}^{-(u-z)} & , \ u \ge z \end{cases} \tag{7}$$

from which the probability that none of these components exceeds a certain value x results:

$$\begin{aligned}\Pr(\max_i u_i \le x|\min_i u_i = z) &= \left(\mathrm{e}^{z} \cdot \int_z^x \mathrm{e}^{-u}\,\mathrm{d}u\right)^{n-1}\\ &= \left(1 - \mathrm{e}^{-(x-z)}\right)^{n-1}\ .\end{aligned} \tag{8}$$

With the definition of PMR (eq. (4)), the CDF of PMR given $z = \min_i u_i$ can be expressed by

$$\Pr(PMR \leq x|z) = (1 - \mathrm{e}^{-z(x-1)})^{n-1} \quad \text{for } x \geq 1,$$

from which the unconditional CDF

$$\Pr(PMR \leq x) = \int_0^{\infty} \Pr(PMR \leq x|z) \cdot f_{\min}(z) \, \mathrm{d}z$$

results:

$$\Pr(PMR \leq x) = n \cdot \sum_{i=0}^{n-1} (-1)^i \binom{n-1}{i} \int_0^{\infty} \mathrm{e}^{-z((x-1)\cdot i+n)} \, \mathrm{d}z$$
$$= \sum_{i=0}^{n-1} (-1)^i \binom{n-1}{i} \frac{n}{(x-1)\cdot i + n}$$

for $x \geq 1$. Thus, the basic CCDF $C_{\mathrm{PMR}}(x)$ for SLM analysis is given by

$$C_{\mathrm{PMR}}(x) = 1 - \sum_{i=0}^{n-1} (-1)^i \binom{n-1}{i} \frac{n}{(x-1)\cdot i + n} \qquad (9)$$

for $x \geq 1$. This result shows that the CCDF $C_{\mathrm{PMR}}(x)$ decays

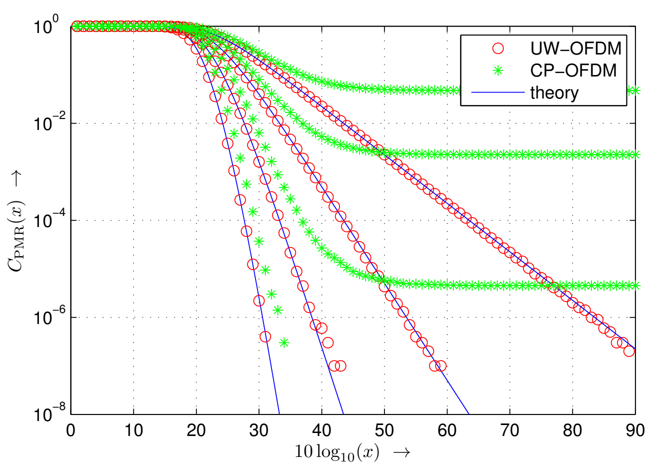

Fig. 7. Analytically derived CCDF $C_{\mathrm{PMR}}(x)$ of peak-to-minimum ratio and SLM and simulations for UW-OFDM as well as CP-OFDM for $V = 1, 2, 4, 8$

for $x \rightarrow \infty$ with x^{-1} down to zero which can clearly by seen from the plot of this function in Fig. 7, i.e. slope -1 in a log-log-scaled diagram. Therefore, generating V variants of a transmit signal in SLM increases the order of decay from 1 to V which indicates that extremely high gains in PMR-R are possible by means of SLM.

In Fig. 7 simulation results are given for PMR-R by SLM for the UW-OFDM system setup given in section 2. It can be seen that the simulation points match the analytically derived CCDF very precisely. Additionally, results for CP-OFDM are given which show a behaviour significantly different from the calculated function. This is caused by the fact that for CP-OFDM it is always possible that (at least) one sample x_i in time domain after IFFT exactly equals zero due to the restriction of the QAM symbols $\tilde{x}_i$ to the set $\{\pm 1, \pm \mathrm{j}\}$,

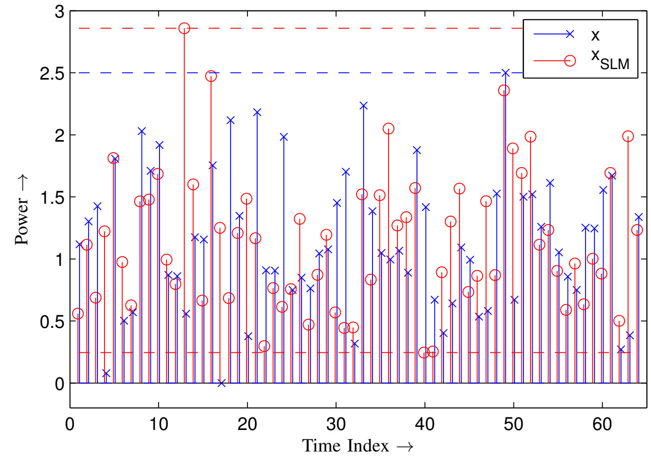

Fig. 8. Snapshot of the power values of the discrete time signals of CP-OFDM with and without SLM for PMR reduction ($V = 16$)

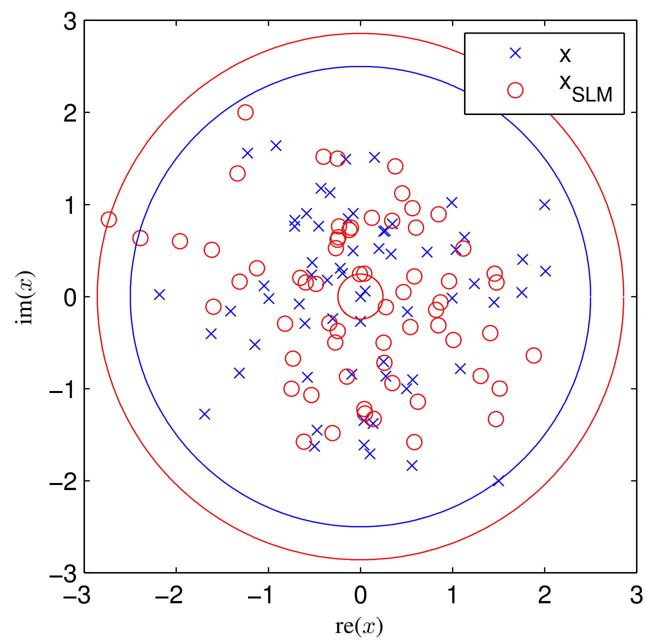

Fig. 9. Scatter plot of the power values of the discrete time signals of CP-OFDM with and without SLM for PMR reduction ($V = 16$)

resulting in a PMR tending to infinity. In contrast, for UW-OFDM the redundant subcarriers $\tilde{r}_i$ are not restricted to a finite set and therefore the probability of zeros in the time domain vector is rather small! Thus, UW-OFDM exhibits a quite better PMR-behaviour than classical CP-OFDM, both, with and without signal shaping. For illustration, Fig. 8 and Fig. 9 show snapshots and a scatter plot, resp., of magnitudes of CP-OFDM frames with and without SLM for PMR-R. The avoidance of very small values can clearly be seen. On the other hand, because very small magnitudes x_i have quite more influence on PMR_v than great ones, pure PMR reduction results in a less efficient PAPR-R.

VII. Conclusion

In this paper we have illustrated that SLM is a just as valid tool for PAPR-R for UW-OFDM as it is for usual CP-OFDM. Also, further examples for another type of signal shaping by means of SLM has been presented, i.e. reduction of the mean energy of symbols at redundant subcarriers and PMR-R. All these features may also be combined in a mixed metric for mapping selection. Thus, the attractivity of UW-OFDM for digital communication is further increased due to efficient signal shaping by SLM.

Acknowledgment

The authors would like to thank the German Research Foundation (DFG) and the Austrian Science Fund (FWF) for supporting this research in project HU 634/9-1 and in project I683-N13, respectively.

References

[1] M. Huemer, C. Hofbauer, J.B. Huber, "The Potential of Unique Words in OFDM", in the *Proc. 15th International OFDM-Workshop*, Hamburg, Germany, 2010, pp. 140-144.

[2] A. Onic, M. Huemer, "Direct versus Two-Step Approach for Unique Word Generation in UW-OFDM", in the *Proc. 15th International OFDM-Workshop*, Hamburg, Germany, 2010, pp. 145-149.

[3] S. Tang, F. Yang, K. Peng, C. Pan, K. Gong, Z. Yang, "Iterative channel estimation for block transmission with known symbol padding - a new look at TDS-OFDM", in the *Proc. IEEE Global Telecommunications Conf. 2007 (GLOBECOM 2007)*, Washington, DC, USA, pp. 4269-4273.

[4] D. Van Welden, H. Steendam, M. Moeneclaey, "Iterative DA/DD channel estimation for KSP-OFDM", in the *Proc. IEEE International Conf. Communications 2008 (ICC 2008)*, Beijing, China, pp. 693-697.

[5] M. Huemer, A. Onic, C. Hofbauer, "Linear Data Estimators for UW-OFDM: Classical and Bayesian Approaches", in the *Proc. 19th European Signal Processing Conf. (EUSIPCO 2011)*, Barcelona, Spain, 2011, pp. 1613-1617.

[6] M. Huemer, A. Onic, C. Hofbauer, "Classical and Bayesian Linear Data Estimators for Unique Word OFDM", in the *IEEE Transactions on Signal Processing*, vol. 59, no. 12, pp. 6073-6085, Dec. 2011.

[7] R. Bäuml, R.F.H. Fischer, J.B. Huber, "Reducing the Peak-to-Average Power Ratio of Multicarrier Modulation by Selected Mapping", *IET Electronics Letters*, vol. 32, pp. 2056-2057, Oct. 1996.

[8] S. Müller, J.B. Huber, "A Comparison of Peak Power Reduction Schemes for OFDM", in the *Proc. IEEE Global Telecommunications Conf. 1997 (GLOBECOM 1997)*, Phoenix, Arizona, USA, pp. 1-5.

[9] M. Breiling, S. Müller-Weinfurtner, J.B. Huber, "Peak-Power Reduction in OFDM without Explicit Side Information", in the *Proc. 5th International OFDM Workshop*, Hamburg, Germany, 2000.

[10] IEEE Std 802.11a-1999, Part 11: Wireless LAN Medium Access Control (MAC) and Physical Layer (PHY) specifications: High-Speed Physical Layer in the 5 GHz Band, 1999.

[11] S.H. Han, J.H. Lee, "An Overview of Peak-to-Average Power Ratio Reduction Techniques for Multicarrier Transmission", in *IEEE Wireless Communications*, vol. 12, no. 2, pp. 56-65, Apr. 2005.

[12] A. Papoulis, S.U. Pillai, *Probability, Random Variables and Stochastic Processes*, 4th ed., New York: McGraw Hill, 2002.

[13] A. Samulak, E. Serebryakova, G. Fischer, R. Weigel, "Modulation and Filter Test Procedure for RF Class-S Power Amplifier Architecture", in the *Proc. IEEE German Microwave Conf. (GEMIC)*, München, Germany, 2009.

[14] M. Huemer, C. Hofbauer, J.B. Huber, "Complex number RS coded OFDM with systematic noise in the guard interval", in the *Proc. Asilomar Conf. on Signals, Systems, and Computers*, Pacific Grove, USA, 2010, pp. 1023-1028.